jove Journal of Visualized Experiments www.jove.com

Video Article

Combining Intravital Fluorescent Microscopy (IVFM) with Genetic Models to Study Engraftment Dynamics of Hematopoietic Cells to Bone Marrow Niches

Lin Wang*[1], Malgorzata M. Kamocka*[2], Amy Zollman[3], Nadia Carlesso[3]

[1]Wells Center for Pediatric Research, Department of Pediatrics, Indiana University School of Medicine

[2]Indiana Center for Biological Microscopy, Department of Medicine, Indiana University School of Medicine

[3]Department of Pediatrics, Indiana University School of Medicine

*These authors contributed equally

Correspondence to: Nadia Carlesso at ncarlesso@coh.org

URL: https://www.jove.com/video/54253
DOI: doi:10.3791/54253

Keywords: Developmental Biology, Issue 121, Myeloid Cells Regeneration, In vivo Imaging, Lineage Tracking, Bone Marrow Niche, Notch signaling, Bone Marrow Transplantation

Date Published: 3/21/2017

Citation: Wang, L., Kamocka, M.M., Zollman, A., Carlesso, N. Combining Intravital Fluorescent Microscopy (IVFM) with Genetic Models to Study Engraftment Dynamics of Hematopoietic Cells to Bone Marrow Niches. *J. Vis. Exp.* (121), e54253, doi:10.3791/54253 (2017).

Abstract

Increasing evidence indicates that normal hematopoiesis is regulated by distinct microenvironmental cues in the BM, which include specialized cellular niches modulating critical hematopoietic stem cell (HSC) functions[1,2]. Indeed, a more detailed picture of the hematopoietic microenvironment is now emerging, in which the endosteal and the endothelial niches form functional units for the regulation of normal HSC and their progeny[3,4,5]. New studies have revealed the importance of perivascular cells, adipocytes and neuronal cells in maintaining and regulating HSC function[6,7,8]. Furthermore, there is evidence that cells from different lineages, *i.e.* myeloid and lymphoid cells, home and reside in specific niches within the BM microenvironment. However, a complete mapping of the BM microenvironment and its occupants is still in progress.

Transgenic mouse strains expressing lineage specific fluorescent markers or mice genetically engineered to lack selected molecules in specific cells of the BM niche are now available. Knock-out and lineage tracking models, in combination with transplantation approaches, provide the opportunity to refine the knowledge on the role of specific "niche" cells for defined hematopoietic populations, such as HSC, B-cells, T-cells, myeloid cells and erythroid cells. This strategy can be further potentiated by merging the use of two-photon microscopy of the calvarium. By providing *in vivo* high resolution imaging and 3-D rendering of the BM calvarium, we can now determine precisely the location where specific hematopoietic subsets home in the BM and evaluate the kinetics of their expansion over time. Here, Lys-GFP transgenic mice (marking myeloid cells)[9] and RBPJ knock-out mice (lacking canonical Notch signaling)[10] are used in combination with IVFM to determine the engraftment of myeloid cells to a Notch defective BM microenvironment.

Video Link

The video component of this article can be found at https://www.jove.com/video/54253/

Introduction

Intravital multiphoton fluorescence microscopy (IVFM) is a powerful imaging technique that allows for the high-resolution, real-time imaging of tissues with depth up to 1mm, depending on the tissue. When applied to the mouse calvarium, it permits observing the behavior of the hematopoietic cells within the BM in a non-invasive manner up to 60-100 μm[11]. This approach is used here to determine the kinetics of engraftment of normal myeloid progenitors in the BM of RBPJ knock-out mice lacking canonical Notch signaling.

Recent work from our group demonstrated that defective canonical Notch signaling in the BM microenvironment leads to a myeloproliferative-like disease[12]. Loss of Notch signaling was obtained by conditional deletion of the DNA binding domain of RBPJ, the critical transcription factor downstream of canonical Notch signaling, using Mx1-Cre induced recombination[10]. In this study, the Mx1-Cre/RBPJ$^{lox/lox}$ mice model was used. Conditional deletion of the DNA-binding motif of RBPJ results in the loss of signaling from all Notch receptors. In the Mx1-Cre model, Cre expression is driven by the Mx1 promoter activated upon administration of polyI:C resulting in the induction of targeted gene deletion in blood cells as well as in stromal components of multiple organs, including BM, spleen and liver.

Mx1-Cre^{+}/RBPJ$^{lox/lox}$ and Mx1-Cre^{-}/RBPJ$^{lox/lox}$ mice induced with polyI:C (hereon indicated as RBPJKO and RBPJWT, respectively) were lethally irradiated and transplanted with normal, wild type hematopoietic cells. Starting from week 4 after transplantation, RBPJKO recipients developed significant leukocytosis followed by splenomegaly. Although RBPJKO mice presented increased percentage of myeloid progenitors in the BM at week 8 after transplant and at later time points, analysis of BM at weeks 4 and 6 did not reveal striking differences in their myeloid cell content compared to control RBPJWT recipients. This observation, together with the fact that Mx1-Cre is expressed in different hematopoietic organs, raised the question whether the BM microenvironment had direct impact on the initiation of the myeloproliferative phenotype.

To determine whether the BM was a critical initial site of disease development, IVFM of the mouse calvarium was used in combination with BM transplantation (BMT), the RBPJ knock-out model, and a lineage tracking system. Transgenic mice expressing EGFP under the control of the specific lysozyme promoter (Lys-GFP)[9] were used to obtain donor cells that could be visualized during BM imaging after BMT. Lysozyme expression is specific to myeloid cells and Lys-GFP marks cells from the common myeloid progenitor (CMP) to the mature granulocyte[13].

IVFM of the BM at different time points demonstrated that Lys-GFP cells homed similarly to the BM of RBPJWT and RBPJKO recipients, but expanded and engrafted faster in the BM of RBPJKO recipients. This difference was dramatic at the earlier time point (week 2) and decreased over time (weeks 4 and 6). However, at these later time points, evaluation of the hematopoietic compartment in the same recipient showed a steady increase in the number of myeloid cells circulating in the PB and localized in the spleen of RBPJKO mice, indicating an increased output of cells from the BM into the circulation. Analysis of Lys-GFP cells localization in the BM of transplanted mice at 6 weeks revealed that myeloid cells were residing further from the vasculature in the RBPJKO microenvironment than in the control.

Collectively, the combination of IVFM with these specific animal models provided insights in the engraftment dynamics of myeloid cells in the RBPJKO BM microenvironment. The experimental design and quantitative approach described here is proposed as a paradigm that can be applied to address similar questions. For example, the use of other cell specific lineage tracking models, such as RAG1-GFP[14] or Gata1-GFP[15] mice, may allow following the behavior of lymphoid or erythroid progenitors, respectively, in the BM.

Protocol

All procedures involving the use of animals were performed with authorization of the Animal Care and Use Committee of Indiana University School of Medicine. Ensure to adhere to the legislation on animal experimentation of the country where the work is performed.

1. Preparation of Mx1CreRBPJ$^{-/-}$ Recipient Mice

1. Cross Mx1-Cre^{+} mice with RBPJ$^{lox/lox}$ mice[10] to obtain Mx1-Cre positive $^{RBPJlox/lox}$ mice[12] and Mx1-Cre negative RBPJ$^{lox/lox}$ littermates to use as controls. Verify the genotype by PCR[10].
2. Use 6-8 week-old Mx1Cre^{+}/RBPJ$^{lox/lox}$ and Mx1Cre^{-}/RBPJ$^{lox/lox}$ mice to perform the polyI:C induction.
3. **Inject polyI:C 200 µg i.p. in Cre^{+} and Cre^{-} mice. Give one polyI:C injection every other day for 3 days the first week. Give one polyI:C injection the second week, 7 days after the previous injection (four injections in total).**
    1. Use RBPJKO (induced Mx1Cre^{+}/RBPJ$^{lox/lox}$) and RBPJWT (induced Mx1Cre^{-}/RBPJ$^{lox/lox}$) mice as recipients 3 weeks after the last polyI:C injection.
    NOTE: It is recommended to use mice induced by pI:pC 3 weeks after injection. The IFNα response triggered by polyI:C induces significant changes in the BM, resulting in the immunophenotypic expansion of HSC and decreased output of mature progenitors into the peripheral blood[16,17]. Representation of the hematopoietic subsets is normalized 3 weeks after injection and the mice can be utilized without the confounding effects of inflammation. This induction protocol has been optimized for RBPJ. If deleting a different gene, the induction protocol may vary depending on the construct, and deletion must be validated. We validated ~100% deletion of the RBPJ region between loxP sites by RT-PCR after a total of four polyI:C injections.

2. Preparation of Lys-EGFP Donor Bone Marrow Cells for Transplantation

1. Euthanize one Lys-EGFP mouse (Carbon dioxide followed by cervical dislocation) 1 or 2 h before the transplant.
2. Spray the animal body surface with 70% ethanol.
3. Use surgical scissors to make a skin incision on both legs around the ankle and with surgical forceps pull away skin and fur together to expose clean muscle tissue.
4. Use surgical scissors to remove as much muscle from the legs as possible. Using a scissors, cut the bones (at the knee and ankle joint) and clean any remaining muscle tissue from the femurs and tibias using gauze sponges. Place the bones (two femurs and two tibias) into a 6-well plate containing DMEM 10% FBS.
5. Crush the bones in a mortar with 10 mL cold 2mM EDTA PBS and pipet the bone marrow cells to bring the cells into single-cell suspension. Alternatively, flush the bones with 2 mM EDTA PBS 3 times from each side with a 1 mL syringe.
6. Filter the bone marrow cells by using a 70-µm filter into a 15 mL centrifuge tube. Rinse filter with 2-3 mL of PBS. Spin the cells down 10 min at 460 x g, resuspend the cells in 10 mL of fresh DMEM 10% FBS.
7. Count bone marrow cells on a hemocytometer and adjust the concentration to 1.5 x 10^7 cells/mL in IMDM without serum. Use 3 x 10^6 cells per animal with a volume of 200 µL. About 1/3 cells of total BM are myeloid GFP+ cells. Leave the cells on ice until ready for injection. Use 0.5 x 10^5 cells to determine GFP expression by FACS[9].

3. Bone Marrow Transplantation of Lys-GFP Cells into RBPJKO Mice

1. Restrain recipient mice in a pie cage. Irradiate mice with a lethal dose of gamma radiation (1,200 Rad) on a Cs 137 irradiator. Use a split dose protocol: 900 rads in the evening followed by 300 rads the next morning (16 h apart).
2. Transplant the lethally irradiated RBPJWT and RBPJKO recipient mice 5-6 h after the second dose of radiation. Inject BM cells harvested from Lys-EGFP mice at a concentration of 3 x 10^6 cells per animal *via* tail vein injection (See details for harvesting cells in section 2).
3. Image independent cohorts of transplanted mice by IVFM at different time points: 24 h, and at weeks 2, 4 and 6, as described below (See section 4 & 5 for *in vivo* imaging procedure).

4. Surgical Preparation for Intravital Imaging

1. Sterilize surgical instruments. Two fine forceps (one straight, one angled), one pair of fine scissors and one pair of needle holders. Prepare operative area with all supplies needed for procedure.
2. Give the mouse an IP injection of ketamine cocktail anesthetic (Xylazine 2.5-5 mg/kg + acepromazine 1.0-2.5 mg/kg + ketamine 90-100 mg/kg) using a 26-28 G needle syringe. Animal will be monitored every 15 min during the procedure and anesthetic will be supplemented as necessary at ¼ of the original dose.
3. Place the mouse on a proper heat source (37 °C heating pad, animal protected from direct contact with heating pad) and visually monitor the respiratory rate.
4. Check reflexes using the toe pinch response. Ensure that the animal is completely under anesthesia before beginning any surgical procedures.
5. Use a 26-28 gauge needle syringe to give mice a tail vein injection of a fluorescent vascular marker (Dextran, 100 µL of 20 mg/mL solution).
6. Apply vet eye ointment to both eyes. Clip the dorsal surface of the animal's head with small electric clippers. Apply a hair removal cream for 5 min. Use gauze sponges to remove the cream and then rinse with saline. Prep the clean scalp with 70% alcohol using a cotton swab.
7. Use fine forceps and scissor to make a small midline skin incision (10-20 mm) on the scalp to expose the underlying dorsal skull surface. Use 5-0 surgical silk to place two stay sutures in the skin on each side of the incision, creating a flap to expose the calvarium for imaging.
8. Position the mice on their back and submerge the exposed scalp in a glass bottom dish filled with microscope oil. Transport the animal to the mutiphoton imaging room.
9. Place the animal on the microscope stage with the calvarium positioned on the glass dish above the objective and then cover with a 37 °C heating pad (animal must be protected from direct contact with heat).

5. In Vivo High Resolution Imaging of the Mouse Calvarium

1. Use an inverted confocal system modified for multiphoton imaging (see **Materials Table**). Following manufacturer's instructions tune a 2-photon laser to 830 nm, place a 20X W, NA 0.95 objective lens in the microscope nose piece and check the laser beam alignment.
   NOTE: Upright microscope systems are most commonly used for these studies, but an inverted multiphoton system may also be utilized. In this study, a custom designed atraumatic stereotaxic device was used. Although there are several commercially available stereotaxic devices for upright microscope systems, there is no commercially available stereotaxic device for an inverted microscope system aimed at securing the mouse skull. As alternative to a custom stereotaxic device, the skull can be secured in position above the objective utilizing various tape or glue methods for stability.
2. Open an image acquisition software. In the "Acquisition Settings" panel check if one directional scanning mode is selected. Set up the speed of scanning to 4 µs/pixel, frame rate to 512 x 512 pixels and zoom to 1.5. Select 20X W Na 0.95 objective from the list of available objective lenses to match the lens positioned in the nosepiece.
3. Access the "Dye List" from the "Image Acquisition Control" panel and select "Two Photon". Open the "Light Path & Dyes" window and select DM690-980 excitation DM. Open the 2P laser shutter by checking the check box in the Laser Unit 2. In the " Microscope Controller" window, select RDM690 mirror.
4. Select " EPI LAMP", choose B/G epi-filter cube and focus the objective onto the specimen to visualize vascular flow and the calvarium bone marrow niche, using as reference the bifurcation of the central vein (a) and the coronary suture (b) (**Figure 2A**).
5. **Collect images using non-descanned mode. Select three external detectors: PMT detector1 to collect SHG signal of collagen (emission filter - 430/100 nm), GaAsP detector2 to collect GFP signal (emission filter - 525/50) and GaAsP detector3 to collect signal of TRITC-dextran (emission filter - 605/90 nm).**
   1. Perform imaging at a scan rate of 4µs/pixel with no averaging to minimize phototoxicity. Collect images at a constant laser power and detector gain adjusted to utilize the full dynamic range of the detector with minimal saturation.
   2. Collect series of sections through the depth of tissue (60 x 1 µm Z-stacks) from 6 regions of calvarium bone marrow. Use step size settings of 1 µm, zoom 1.5 and 512 x 512 pixels frame size (423 µm x 423 µm).
      Note: Overall total time required to image one mouse is 1-1.5 h.

6. Quantitative Analysis

1. Perform the image quantitation and 3D reconstructions using a dedicated 3D/4D image quantitation and visualization software as per manufacturer's instructions (see **Materials Table**). Visualize interactively Z-stacks in 3D utilizing Maximum Intensity Projection (MIP), alpha-blend or shadow projection volume rendering algorithms.
2. Segment GFP cells using the "*Spot Object segmentation module"*. Apply stack arithmetic processing (channel subtraction) to eliminate false positive count of GFP cells (this eliminates signal of bone cells displaying strong fluorescence in green and red channels).
3. Perform segmentation of vasculature and bone surface using the Surface segmentation module. If required, calculate distances of cells to any of the above surfaces by applying X-tension algorithms called "distance of spot to surface".

Representative Results

Cohorts of 2 RBPJKO and 2 RBPJWT recipients were imaged in an individual imaging session at different time points: 24 h and 2, 4 and 6 weeks after transplantation of BM Lys-GFP cells (workflow is illustrated in **Figure 1A**).

In each mouse, images were acquired from 6 standard regions of the BM calvarium, identified by their position in relation to the bifurcation of the central vein (**Figure 2A**, **a**) and the coronary suture (**Figure 2A, b**). Injection of Dextran Texas-Red prior to imaging allows the identification of these landmarks and the selection of 6 regions (**Figure 2A**): Upper Left, Medium and Right (UL, UM, UR), and Lower Left, Medium and Right (LL, LM, LR). 60 x 1 µm z-stacks are collected from each region and rendered as 3-D Maximal Intensity Projection (MIP), (**Figure 2B**); 3-D Shadow Projection, which includes the bone component (gray) generated by the second harmonic generation (SHG) microscopy probing collagen organization (**Figure 2C**); and finally, a 3-D Segmented image, which allows quantitation of cells and measurement of their distances from the bone and the vessels (**Figure 2D**).

Because of potential differences in homing preferences of hematopoietic cells in the different regions of the BM calvarium after transplant, it is important to sample multiple regions in the calvarium of each mouse. **Figure 3** shows an example of cell distribution in the 6 regions analyzed in one RBPJWT and one RBPJKO recipient at 2 weeks after BMT (green - myeloid cells, gray-bone) using shadow projection 3D rendering algorithm. Number of cells per region ranged from 64 to 258 in the RBPJWT mouse and from 265 to 573 in the RBPJKO mouse. Final results are then expressed as average number of the 6 regions analyzed: number of cells per region / per mouse (average 135 in RBPJWT vs 469 in RBPJKO). This representative experiment indicates that there is a larger variation in cell distribution per region in the RBPJWT than in the RBPJKO recipient. Furthermore, in addition to the variation found in the calvarium regions within a mouse, which is common, there are variations among individual mice within the same group. Thus, it is important that for each time point at least 4 mice are evaluated per experiment to obtain a minimum of a total 24 to 30 regions to be analyzed per condition.

Figure 4 shows the dynamics of myeloid progenitor expansion in a Notch defective BM microenvironment compared to control over 6 weeks after transplantation. In this representative experiment, 8 RBPJWT and 8 RBPJKO mice were transplanted and imaged at the indicated time points (2 RBPJWT mice and 2 RBPJKO mice at each time point). **Figure 4A** shows a representative 3-D reconstruction of 1 out of 6 regions acquired. Cells in each of the 6 regions were counted and the average number of cells/region of two mice at each time point (total 12 regions) was calculated for RBPJWT and RBPJKO recipients (**Figure 4C**). This analysis indicates that: (i) donor Lys-GFP cells in RBPJWT and RBPJKO recipients have a similar homing efficiency; ii) cells in the RBPJKO recipients expand more rapidly and are twice the number of cells in the RBPJWT recipients at week 2 after BMT; iii) cells in RBPJWT recipients expand later and are 2-fold higher than cells in RBPJKO recipients at week 4 after BMT; and iv) cell number in both RBPJWT and RBPJKO recipients become similar at week 6 after BMT. Analysis of donor myeloid cells in the PB indicates a higher output of myeloid cells from the BM of RBPJKO recipients than from the BM of RBPJWT recipients at week 4, at the time when the BM of RBPJKO mice showed a lower content of Lys-GFP cells. The combined analysis of myeloid cells resident in the BM and of myeloid cells circulating in the PB, indicate that in the RBPJKO BM microenvironment Lys-GFP cells expand and are ready to mobilize more rapidly. Parallel FACS analysis of Lys-GFP cells in long bones BM from the same mice showed a trend similar to the one observed by IVFM; however, differences between conditions were less pronounced (**Figure 4B**).

Measurement of the distance of individual Lys-GFP cells from the bone or the vasculature is shown in **Figure 5**. In this representative study, 3-D segmentation analysis of the LM region of RBPJWT and RBPJKO calvarium at 6 weeks from BMT was used (**Figure 5A**). Distance from bone and the vessels were calculated for each cell in the region: 200 cells in RBPJWT and 255 cells in RBPJKO, and thus, expressed as an average. The analysis shows that Lys-GFP cells localize at a similar distance from the bone in the RBPJWT and RBPJKO mice (11 µm), but that they reside more distant from the vasculature in RBPJKO mice than in RBPJWT mice (15 µm *vs* 5 µm, respectively). This result is intriguing, as in the RBPJKO mice Lys-GFP cells mobilized into the circulation more than in RBJWT mice, and would thus be expected to localize closer to the vessels. However, it is possible that the difference in localization reflects a different stage of differentiation of these two populations (in RBPJWT and RBPJKO), a point that cannot be addressed by this analysis. The significance of this result will be followed-up with a larger pool of cells in all 6 regions and by combining FACS analysis.

Overall, suboptimal results are obtained when a small number of regions are analyzed per mouse. Imaging is particularly challenging at the early time points following BMT, as lethal irradiation damages the vasculature and leakage of dextran from capillaries reduces image definition. Thus, it is important to have a large number of repetitions, especially at the earliest time points.

SHG is a useful tool for investigating collagen fiber organization in 3D. It is a second-order nonlinear optical process which originates from structures such as collagen fibers possessing non-centrosymmetry and a high second-order nonlinear coefficient. When intense incident light interacts with such structures, it generates light at twice the incident frequency or half the incident wavelength. Therefore, no labeling is needed in order to capture SHG signal during 2-photon microscopy. With 830 nm excitation wavelength, we capture SHG signal in the blue channel with emission filter 430/100 nm.

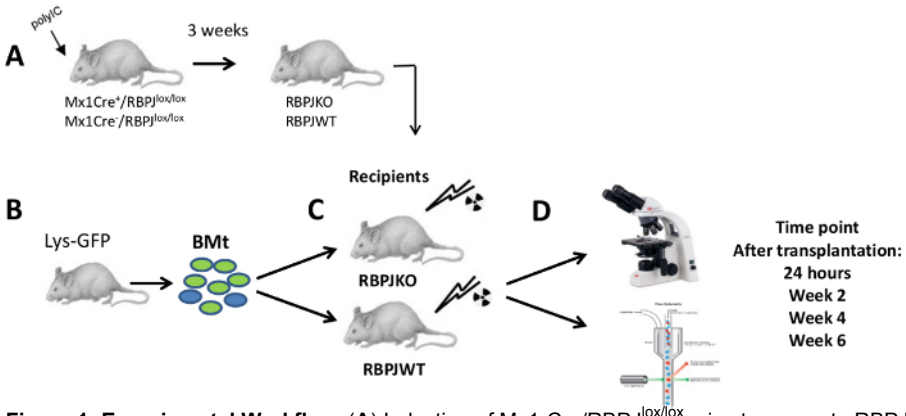

Figure 1: Experimental Workflow. (**A**) Induction of Mx1-Cre/RBPJ$^{lox/lox}$ mice to generate RBPJKO and RBPJWT mice ~4 weeks prior imaging; (**B**) Preparation of BM cells from Lys-GFP transgenic mice; (**C**) Transplantation of BM Lys-GFP cells into lethally irradiated RBPJKO or RBPJWT recipients; (**D**) IVFM of mouse calvarium at 24 h, 2, 4 and 6 weeks after BMT, followed by euthanasia and BM analysis by FACS. Please click here to view a larger version of this figure.

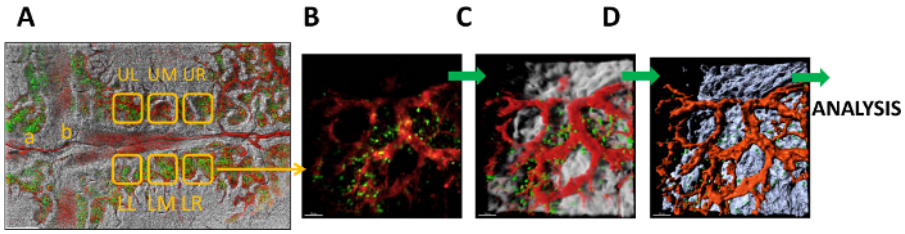

Figure 2: IVFM of the BM Vascular Niche. (**A**) Mosaic multi-photon image of Lys-EGFP mouse calvarium showing the 6 standard regions of imaging (UL: upper left, UM: Upper middle, UR: Upper right, LL: Lower left, LM: Lower middle, LR: Lower right) (green, myeloid cells; red, vasculature; gray, bone) 10X magnification; (**B**-**D**) BM niche detail rendered as: (**B**) MIP, (**C**) 3-D Shadow Projection, (**D**) 3-D Segmentation image. Images were processed -using a dedicated 3D/4D image quantitation and visualization software (Table 1). Scale bars = 50 µm in B, C, D. Please click here to view a larger version of this figure.

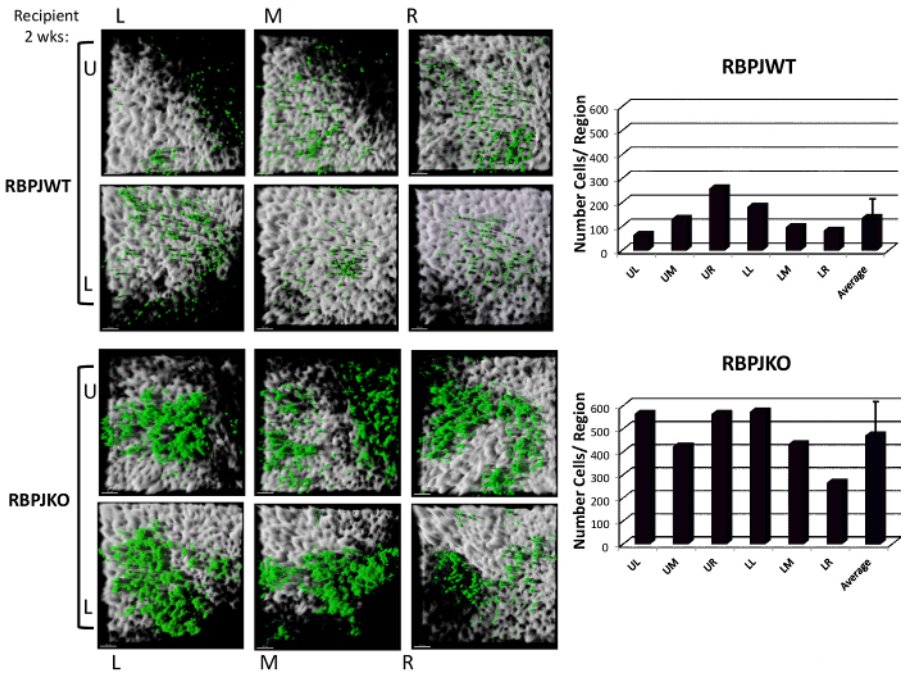

Figure 3: Myeloid Cells Engraftment at Week 2. Images of Lys-GFP cells (green) and bone surface (gray) in the 6 BM regions from the calvarium bone of one RBPJWT and one RBPJKO mouse (U: Upper, L: left, M: Middle, R: Right). Scale bars = 50 µm. Bar graphs (right) indicate the number of cell counted in each region (RBPJWT range 64-258; RBPJKO range 265-573) and their average number 135 STD+/-73, and 469 STD +/- 121. Please click here to view a larger version of this figure.

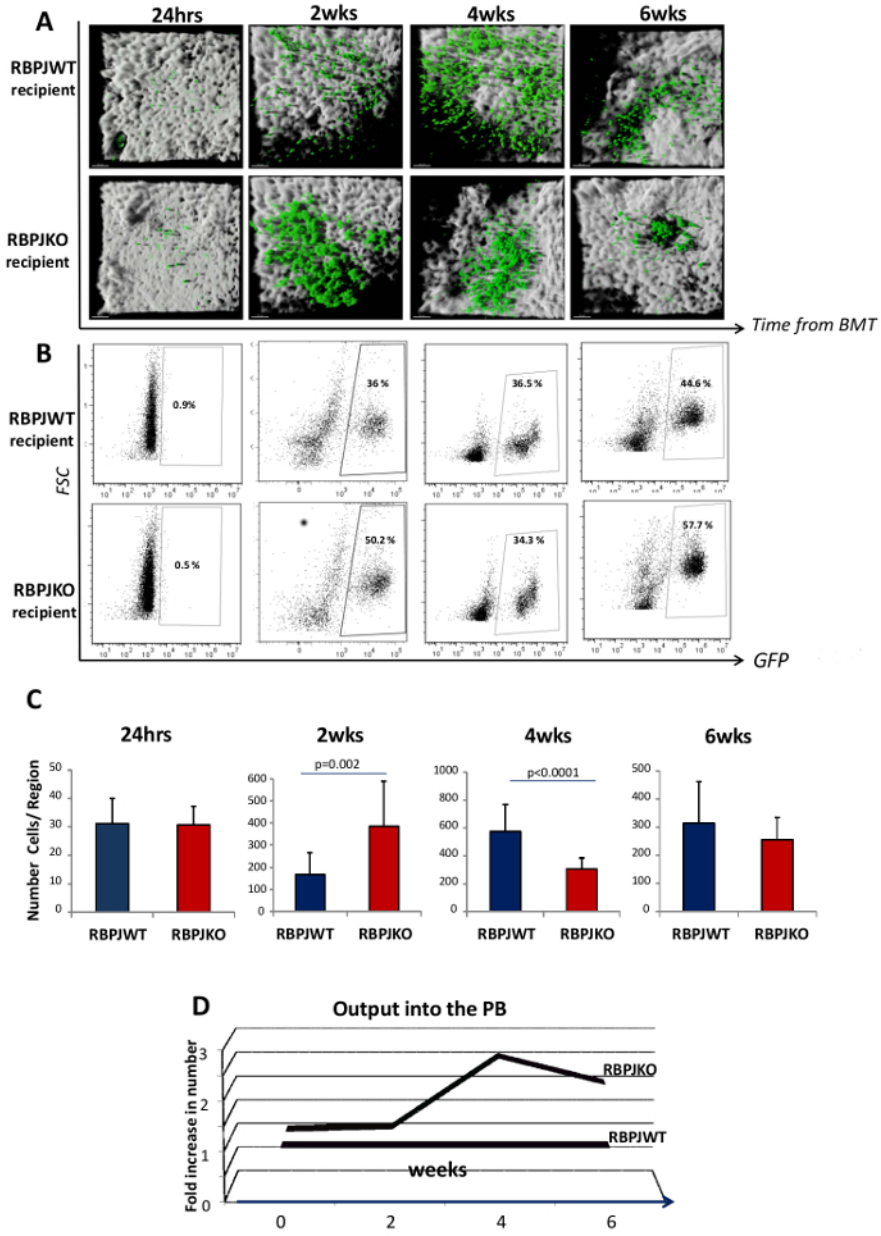

Figure 4: Kinetics of Myeloid Cells Engraftment and Output Following BMT. (**A**) Images of Lys-GFP cells (green) and bone surface (gray) in one representative region from the calvarium of one RBPJWT and RBPJKO mouse at each of the time points indicated. Scale bars = 50 µm; (**B**) Dot blots show percentage of Lys-GFP positive cells by flow cytometry within the BM of long-bones harvested from the same mouse imaged in vivo (above). (**C**) Bar graphs indicate average number of cells/region in 2 mice (total 12 regions) at each time point, +/- STD. (**D**) Line graph shows fold increase in the total number of neutrophils (enumerated by cell counter) presented in the PB of the same mice than in (A) at the indicated time points. Please click here to view a larger version of this figure.

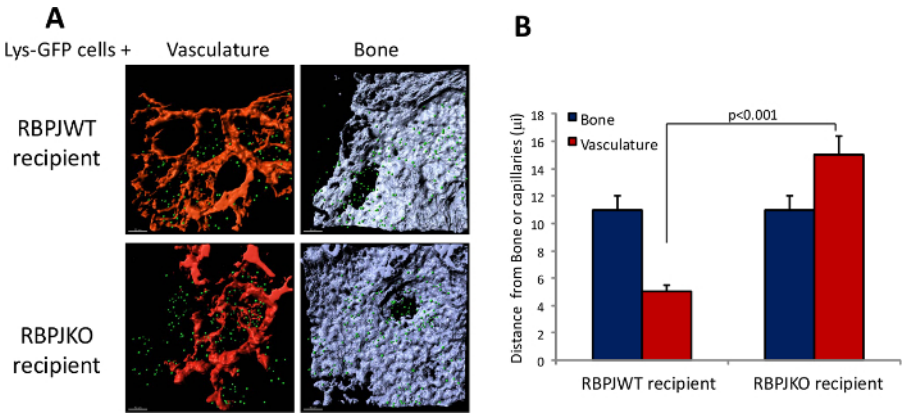

Figure 5: Localization of Myeloid Cells in the BM Relative to the Bone and to the Vasculature. (**A**) Representative 3-D segmented images of Lys-GFP cells and vasculature, and Lys-GFP cells and bone in the same region of calvarium bone in RBPJWT and RBPJKO recipients at week 6 from BMT. Scale bars = 50 µm. (**B**) Bar graph summarizes the average distance in µm +/-SEM of Lys-GFP cells from the bone surface or the vasculature. Number of cells measured in: RBPJWT n = 200 cells and RBPJKO n = 255 cells. Distance of Lys-GFP cells from the vasculature is greater in RBPJKO than RBPJWT mice, p <0.001 (Student's t-test). Please click here to view a larger version of this figure.

Discussion

This protocol describes an experimental design optimized to study the kinetics of hematopoietic cells engraftment by Intravital Florescent Microscopy. In this study, the expansion of myeloid progenitor cells in a WT BM or in a Notch signaling defective BM was tracked in the bone calvarium by following Lys-GFP positive myeloid cells after BMT into RBPJWT or RBPJKO recipients. This approach is proposed as a model that can be applied to address similar questions, for example: i) to determine the expansion and localization in the BM niches of cells of other lineages, such as lymphoid, erythroid or megakaryocytic cells, by using as donor cells hematopoietic cells carrying lineage specific promoters driving GFP or Tomato-red; ii) to assess different micro-environmental determinants by using other specific KO or transgenic mice as recipients.

Strength of this imaging protocol in the calvarium bone, is that the anatomic landmarks used to select the BM regions, bifurcation of the central vein and the coronary suture, are reasonably conserved in all mice, permitting consistency between individual experiments while forgoing the requirement of an automated stage. In addition, the use of the GFP model to track hematopoietic cells proved to be very effective, as GFP provided a stable signal in suboptimal conditions, such as after irradiation. Finally, the imaging set-up described, using an inverted microscope and a customized stereotaxic device in which the mouse is in supine position, greatly minimize breathing artifacts.

Two aspects of this experimental design, if implemented, could lead to a broader and more effective use of IVFM of the calvarium. First, it will be important to optimize and standardize protocols of longitudinal imaging allowing the observation of the same mouse at different time points (from day 2 to several weeks) after intervention (*i.e.* BMT or therapy) instead of using independent cohorts of mice. As this approach requires appropriate conditions for post-surgery recovery and the use of measures to counteract inflammation, infection, and scar formation at the site of imaging, its application is currently limited. Second, it will be valuable to develop an array of lineage tracking mouse models carrying fluorescent proteins in specific cells of the BM niche (vascular, endosteal, perivascular and neuronal) to combine hematopoietic cell functions with specific characteristics of the BM niches.

Imaging of bone still has some challenges and limitations compared to other tissues. Although the two-photon microscope can penetrate 100-1,000 micron deep in tissues, it is still challenging to image through the entire thickness of the calvarium bone. Images lose quality with increasing depth so the protocol here describes reliable analysis of BM regions from 60 micron thick stacks. Another factor that can result in inconsistency or suboptimal imaging is the curved shape of the calvarium bone, which can bring the image out of focus. It is crucial to have the skull positioned perfectly on the glass dish above the objective, possibly with a stereotaxic device. Indeed, the skull size is important: skull of mice too young or too small may not fit perfectly in a given stereotaxic device. As an example, the device utilized here does not fit mice younger than 6 weeks and less than 20 g.

An additional limitation is that the imaging system utilized in this study is limited to 3 channels. As the blue channel is automatically assigned to collect non-labeling based SHG signal of the bone collagen, only 2 channels are available for specific fluorescence labeling. Furthermore, this system has a speed limitation of 1 frame/s at 2 µs/pixel dwell time and 512 x 512 pixels frame size, which is not ideal for fast dynamic processes (such as measure of blood flow and evaluation of cell mobilization in the blood stream).

A significant challenge is that the irradiation performed for BMT compromises the integrity of vasculature. The vascular leakage present in the BM after irradiation causes difficulties with segmentation/quantitation of individual structures, which can pose difficulty in the quantitative analysis.

Finally, it is important to consider that imaging of one mouse takes approximately 1 h, and the number of mice that can be imaged in a given day is limited (~4 to 6 mice). Thus, increase in sample size to obtain power of analysis may require multiple independent experiments, which can increase variability.

Following this protocol, the number of hematopoietic cells Lys-GFP^{+} cells detected by IVFM in the BM after 24 h from BMT is ~30 cells/region and it is quite a small number compared to the initial input of cells (3 x 10^{6}). Although, part of this problem is due to cell trapping in lung and liver

before homing to the BM following i.v. injection, it remains to be explored whether there are regions in the calvarium other than the ones selected where the transplanted cells home at higher efficiency.

Homing and engraftment of cells into the BM after BMT are commonly followed by flow cytometry by measurement of CD45.1/CD45.2 markers, GFP, Carboxyfluorescein succinimidyl ester (CFSE) or combination of lineage and stem cell markers. The use of IVFM, especially at early time points, makes available unique and additional information that cannot be provided by flow cytometry. For example, often it is not easy to distinguish by FACS events that are "cells" from events that are "artifacts", in particular when a low number of positive events is collected (*i.e.* at 24 h from BMT). IVFM provides information on morphology and localization of the cells that aids this distinction. Similarly, FACS analysis of BM hematopoietic cells harvested by flushing or crashing the bones will include cells that were residing in the niche and cells that were already in circulation in the vascular system. Indeed, IVFM permits the distinction and evaluation of cells resting within the BM niche and cells that are mobilizing into the bloodstream. This distinction is of great value when studying the kinetics of homing, localization, differentiation and mobilization in a given model. Importantly, IVFM can provide unique information on the position of the hematopoietic cells relative to the microenvironment cells constituting a specific niche.

Other methods used to address the composition of the BM niche, such histological analysis have been used. Comparison between intravital microscopy of the BM and histological analysis by confocal microscopy has been thoroughly and elegantly discussed by Lo Celso *et al.*[18].

Disclosures

The authors have nothing to disclose.

Acknowledgements

Imaging was carried out in the Indiana Center for Biological Microscopy at Indiana University, directed by Dr. Ken Dunn. The stereotaxic device is a prototype designed and made by Mark Soonpaa, Wells Center for Pediatric Research. This work was supported by NIH/R01DK097837-09 (NC), NIH/R01HL068256-05 (NC), NIH/NIDDK1U54DK106846-01 (NC), the MPN research Foundation (NC) and the CTSI Collaborative project IUSM/Notre Dame (NC).

References

1. Carlesso, N., & Cardoso, A. A. Stem cell regulatory niches and their role in normal and malignant hematopoiesis. *Curr Opin Hematol.* **17** (4), 281-286. (2010).
2. Lo Celso, C., & Scadden, D. T. The haematopoietic stem cell niche at a glance. *J Cell Sci.* **124** (Pt 21), 3529-3535 (2011).
3. Calvi, L. M. *et al.* Osteoblastic cells regulate the haematopoietic stem cell niche. *Nature.* **425** (6960), 841-846 (2003).
4. Kiel, M. J., Yilmaz, O. H., Iwashita, T., Terhorst, C., & Morrison, S. J. SLAM family receptors distinguish hematopoietic stem and progenitor cells and reveal endothelial niches for stem cells. *Cell.* **121** (7), 1109-1121 (2005).
5. Zhang, J. *et al.* Identification of the haematopoietic stem cell niche and control of the niche size. *Nature.* **425** (6960), 836-841 (2003).
6. Mendez-Ferrer, S. *et al.* Mesenchymal and haematopoietic stem cells form a unique bone marrow niche. *Nature.* **466** (7308), 829-834 (2010).
7. Naveiras, O. *et al.* Bone-marrow adipocytes as negative regulators of the haematopoietic microenvironment. *Nature.* **460** (7252), 259-263 (2009).
8. Scheiermann, C. *et al.* Adrenergic nerves govern circadian leukocyte recruitment to tissues. *Immunity.* **37** (2), 290-301 (2012).
9. Faust, N., Varas, F., Kelly, L.M., Heck, S., Graf, T. Insertion of enhanced green fluorescent protein into the lysozyme gene creates mice with fluorescent granulocytes and macrophages. *Blood.* **96** (2), 716-726, (2000).
10. Han, H. *et al.* Inducible gene knockout of transcription factor recombination signal binding protein-J reveals its essential role in T versus B lineage decision. *Int Immunol.* **14** (6), 637-645 (2002).
11. Lo Celso, C. *et al.* Live-animal tracking of individual haematopoietic stem/progenitor cells in their niche. *Nature.* **457** (7225), 92-96 (2009).
12. Wang, L. *et al.* Notch-dependent repression of miR-155 in the bone marrow niche regulates hematopoiesis in an NF-kappaB-dependent manner. *Cell Stem Cell.* **15** (1), 51-65 (2014).
13. Miyamoto, T. *et al.* Myeloid or lymphoid promiscuity as a critical step in hematopoietic lineage commitment. *Dev Cell.* **3** (1), 137-147 (2002).
14. Luc, S. *et al.* Down Regulation of Mpl marks the transition to lymphoid-primed multipotent progenitors with gradual loss of granulocyte-monocyte potential. *Blood* **111** (7), 3424-3434 (2008).
15. Suzuki, M., Moriguchi, T., Ohneda,K., Yamamoto, M. Differential contribution of the Gata1 gene hematopoietic enhancer to erythroid differentiation. *Mol Cell Biol.* **29** (5), 1163-1175 (2009).
16. Essers, M.A. *et al* IFNalpha activates dormant haematopoietic stem cells in vivo. *Nature.* **458** (7240), 904-908 (2009).
17. Pietras, E.M. *et al* Re-entry into quiescence protects hematopoietic stem cells from the killing effect of chronic exposure to type I interferons. *J Exp Med.* **211** (2), 245-262 (2014).
18. Scott, M. K., Akinduro, O., & Lo Celso, C. In vivo 4-dimensional tracking of hematopoietic stem and progenitor cells in adult mouse calvarial bone marrow. *J Vis Exp.* (91), e51683 (2014).

